

PAPER • OPEN ACCESS

## Design and development of wireless networking for solar PV panel cleaning robots

To cite this article: G Anilkumar *et al* 2020 *IOP Conf. Ser.: Mater. Sci. Eng.* **937** 012024

View the [article online](#) for updates and enhancements.

 **240th ECS Meeting**  
Oct 10-14, 2021, Orlando, Florida

**Register early and save  
up to 20% on registration costs**

Early registration deadline Sep 13

**REGISTER NOW**



# Design and development of wireless networking for solar PV panel cleaning robots

**G Anilkumar<sup>1\*</sup>, K Naveen<sup>2</sup>, M T V S H K Pavan Kumar<sup>3</sup>, G V Brahmendra Kumar<sup>4</sup>, K Palanisamy<sup>5</sup>, Avinash Patil<sup>6</sup>, Deepak Sachan<sup>7</sup>**

<sup>1,2,3</sup>School of Renewable Energy, JNT University, Kakinada, 533003, India.

<sup>4,5</sup>Centre for Smart Grid Technologies, Vellore Institute of Technology, Vellore, 632014, India.

<sup>6,7</sup>Technology Development Lab, BHEL R&D Division, Hyderabad, 500093 India.

Email: [koreddinaveen@gmail.com](mailto:koreddinaveen@gmail.com), [mahantpavankumar@gmail.com](mailto:mahantpavankumar@gmail.com), [brahmendrakumar.g@gmail.com](mailto:brahmendrakumar.g@gmail.com), [kpalanisamy@vit.ac.in](mailto:kpalanisamy@vit.ac.in),

[avinashp@bhel.in](mailto:avinashp@bhel.in), [deepaksachan@bhel.in](mailto:deepaksachan@bhel.in)

\*Corresponding author: [gorantlaanilkumar@gmail.com](mailto:gorantlaanilkumar@gmail.com)

**Abstract.** This paper discusses about one of the possible solutions to overcome the influence of dust on the surface of solar PV panel. A decrease in power output with the increase in particle deposition has been identified in large scale solar PV power generation where there were many numbers of solar panels connected in the form of arrays and each array requires a robot to carry out efficient cleaning with in stipulated time. Autonomous automatic cleaning operation along with self-control and monitoring of accumulated dust with proper coordination through networking between robots is prerequisite option to attain efficient cleaning system in large scale solar power plants. To accomplish the same, selection of appropriate communication technology for real time wireless networking of solar cleaning robots with low power consumption and data delay to operate over wide area is required. Here an attempt had been made to bring in an automated robot cleaning system using low power wide area network (LPWAN) based on a network of ESP 8266 Node MCU's associated with a set of sensors under different configurations which showed successful results for implementation in industrial scale large solar PV power plants.

## 1. Introduction

Allocation Operation and Maintenance of solar photovoltaic (PV) panels should be carried out frequently not only to improve its efficiency but also to prevent the damage caused by the accumulated dust due to environmental pollution. The main influence that exhibit impact on operating parameters is PV panel efficiency. There is a dire need to explore technical solution to this problem in an efficient manner although there were some existing methods. A study on several dust removal techniques has been carried out for example [1,2] which suggested that removal of dust particles from the surface of solar PV panel can be done by using nylon brush with automated robotic system where as [3] mentioned about the energy losses

that arise due to deposition of dust particles on solar panel. A significant amount of power loss was noticed by the research work carried out by earlier researchers [1-4]. In case of PV bases large scale power generation, the intensity of power loss further increases. Classification of solar PV cleaning mechanisms are presented in figure 1 which shows a glimpse of several methodologies and techniques such as natural cleaning, mechanical cleaning, self-cleaning and electrostatic cleaning that are available in the market to remove the accumulated dust on the solar PV panel. Here, an attempt had been made to develop an automated cleaning system using low power wide area network (LPWAN) based on a network of ESP 8266 Node MCU's associated with a set of sensors under different configurations which showed successful results for implementation in industrial scale large solar PV power plants.

The efficiency of the solar PV panel has reduced to 40% after one year of solar system installation [5]. The reasons that are attributed were due to high temperature, panel pitch and orientation [6], accumulation of dust, snow, sea salt and bird droppings [7]. Among those, the accumulation of dust and other particles on the solar PV panel reduces the system efficiency of the panel about 50% [8]. Moreover, these particles can be removed from the surface of the panel by providing proper cleaning mechanism. Few research studies were carried out to deploy different software-based prototype cleaning mechanisms. By implementing arm controller and gear motor-based cleaning method, the output increased about 35% [7]. A microcontroller based automatic dust cleaning system was developed to increase the panel efficiency of about 1.6% to 2.2% by cleaning the panel every two hours [9-15]. By providing a self-cleaning mechanism with software and hardware, the operating cost reduces and the overall efficiency can be increased [16-25]. From the simulation, the accumulated dust on the panel can be detected and provide the cleaning mechanism which increases the performance of the cleaning mechanism [26-30]. A dust cleaning mechanism with a panel cooling system showed an improvement in the performance of the PV panel [31-34]. An automatic dust cleaning system operated during the day time and turned off during night time for solar street light panels showed an increase in the overall system efficiency [35]. Among the above discussed research studies, it has been identified that, most of the developed or proposed automated cleaning system were implemented with dry cleaning mechanism to avoid the panels from short circuits and allowed to operate when dust was accumulated on the panel.

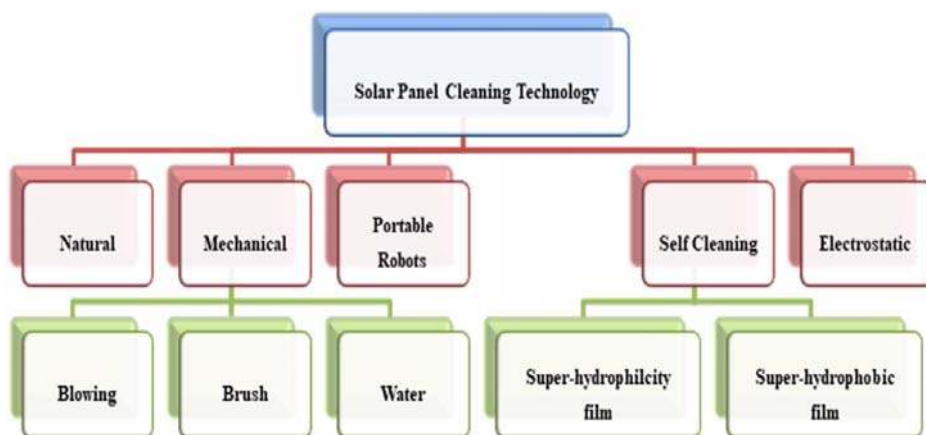


**Figure 1.** Solar PV panel cleaning methods.

## 2. Cleaning robot for industrial solar panels (CRISP)

### 2.1 Construction

Figure 2 represents the recently developed CRISP robot at BHEL R&D, Hyderabad. The solar PV panel cleaning robot is designed in a modular fashion with two-axis movement in X and Y direction on the

edges of the panel. It has a long aluminium guide rail along the modular frame which allows the robot to move along the horizontal direction with a set of motorized dummy wheels that can travel on top and bottom edge of the solar panel eliminating the capital investment of additional rails in addition to a cleaning trolley with a pair of rotating microfiber brushes that can move up and down in vertical direction by making use of motorized winch and a wire rope to clean the surface of the solar PV panel. An IR sensor and DC motor is used to adjust the height of cleaning brushes. Proximity sensors are used to detect the top and bottom position of the cleaning trolley for automatic up and down movement. Limit switches are used to detect the start, end, and position of the robot. Distance between the microfiber brush and solar panel surface is adjustable. The robot is parked in a parking station where its batteries are automatically charged by an independent solar panel in the day time and during the night time, the robot cleans the solar panels. The robot is controlled by a PLC controller. An android based application or web-based application is used as HMI for controlling the robot.



**Figure 2.** CRISP.

## 2.2 Mechanical Design

The construction of the CRISP can be categorized in two ways those are mechanical design and electrical control design. The mechanical design of the CRISP comprises of top drive, bottom drive, rope winch, trolley, parking station. The top drive of the CRISP consists of two motorized wheels which are fixed at the right and left side of the top extrusion bar. The right-side motorized wheel can be coupled to the rotary encoder which is used for monitoring the accurate distance traveled by the robot. The top extrusion bar also consists of four dummy wheels which are used to provide support to the robot. The bottom drive also consists of two motorized wheels which are fixed at the left and right side of the bottom extrusion bar. It consists of a rotary encoder which is used to control the speed of the robot. The winch is one of the major components involved in the cleaning cycle by which the trolley with brushes is moved up and down for cleaning the solar panels. Two motors are coupled to the winch pulley which rotates by winding and unwinding the wire rope of the trolley around the pulley. The trolley is fixed with two brushes to carry out the cleaning operation of the solar panels. These brushes are coupled to the motors which are fixed on one side of the trolley. For efficient cleaning of the panels, the height of the brushes can be adjusted according to the solar panel positioning. The trolley is based on the main frame of the robot on free running wheels and movement of the trolley is made possible through the wire rope of which one end is tied to the trolley and the other end to the winch pulley at the top. The parking station consists of a solar panel with charge controller and hard stops for mechanical stop and electrical contact. This station provides the parking

facility to the robot. It also consists of parking cover which is made with nylon used to protect the robot trolley from rain and UV rays. It provides the charging facility to the robot batteries during the presence of solar radiation through the electrical contacts which are mounted on the mechanical hard stops.

### 2.3 Electrical Design

Electrical control design of CRISP comprises of PLC and extension module, solar panel, charge controller, rechargeable battery, 12 V high torque dc motors, Wi-Fi router, 12/24 V DC-DC converter, 7805 voltage regulator, dual DC motor driver, digital DC volt & ammeter, rotary encoder, limit switch, proximity sensor, current sensor, rain sensor, DHT11 sensor, panel lamp indicators, emergency push button switch. Using preprogrammed simulation program, PLC controls the speed and direction of the motors (such as top drive, bottom drive, winch, and trolley brush motors) with proximity sensor, photo eye sensor, limit switch, encoder, rain sensor, current sensor and potential divider as an input. It can transfer the signal to the Wi-Fi router through the category 5 Ethernet cable for control and monitoring of the robot with Wi-Fi connected devices (such as mobile, laptop, tab, etc.). A transistor I/O module is connected to this PLC to extend the number of inputs and outputs. While the above mentioned sensors and electronic devices will carry out their usual functions in the system design, CRISP robot is equipped with a dedicated self-cleaning solar PV panel with 120 Wp maximum peak power, 19.95 V maximum output voltage, 23.26 V of open circuit voltage, 6.02 A maximum current output, 6.36 A of short circuit current that can be wired to attain a maximum system voltage of 600 V had been selected to charge two parallel connected 12V-24 Ah lead-acid batteries during day time through charge controller.

### 2.4 Working

Initially, the robot would be at home position in the parking station provided, where the batteries of the robot get charged from its own solar panel through a charge controller. By considering the shadow effect of the robot on the solar panels, the robot is made to be idle during the sun hours of the day and made to start the cleaning cycle during the non-operative hours of the solar panels. The movement of the robot can be considered as a two axes movement, where the cleaning of the panels is done in the vertical movement of the trolley, while the robot moves in forward and backward direction in the horizontal movement covering the entire area of the array of the solar panels. The cleaning cycle can be considered in four phases viz., Upward movement, Downward movement, Forward movement, and Backward movement.

During the Upward movement, the trolley is pulled up by the winch with the brushes rotating resulting in the dust being wiped off from the panel surface. This upward movement will take place until the top proximity sensor gets activated. Once the sensor senses the trolley at the top, the winch changes the direction unwinding the wire rope which results in the downward direction of the trolley.

During the Downward movement, the dust wiped off in the upward direction is completely pushed downward with the brushes and is pushed out of the panel surface making the panel surface completely clean. The downward movement takes place until the bottom proximity sensor is activated. Once the sensor is activated, the winch and the brushes stop rotating and the robot is ready to move in the forward direction.

During the Forward movement, the robot is supposed to move forward as the cleaning is done in that particular position. Now the robot has to move a distance which is equal to the length of the brush since the cleaning done is for one length of the brush. This is achieved by programming a set number of counts for the encoder. As there are separate encoders for top and bottom drive, the robot moves until both drives are moved for set length. This eliminates any tilt in the movement of the robot due to an imbalance in the load. Once both the drives move for the set number of counts, the cleaning starts in the upward direction and downward direction. Once cleaning is done again, the robot moves in the forward direction. This takes place till the top and bottom forward limit switches are on. Once the top and bottom forward limit switches are on, the last upward and downward movements are done for the last time and the top drive and bottom drive change their direction.

During the Backward movement, the robot comes to the home position at the parking station as the top drive and bottom drive move in a backward direction until the top and bottom backward limit switches are on. Once these limit switches are on, the robot contacts the charge controller which is connected to the solar panel and the batteries get recharged until the next cleaning cycle starts. It can be operated in manual mode also by pressing respective switches to move left, right, up, down and trolley brushes.

### 3. Wireless networking of CRISP

Wireless network resembles a set of devices that can be interconnected based on certain communication methodologies and techniques without using wires. Here in this case, devices refer to robots that are used for solar panel cleaning mechanism which can be grouped together wirelessly and form a wireless local area or wireless wide area network (WLAN or WWAN). Coordinated control and monitoring can be attained in-between robots and the HMI from a central control station to enhance the system performance. A PLC along with Wi-Fi router can be used in CRISP to accomplish the same. But a PLC with Wi-Fi option is not economically viable in addition to excess power consumption. Instead, an ESP 8266 NodeMCU microcontroller unit with inbuilt Wi-Fi antenna can be considered that allows access point as well as device control capability to HMI to attain desired wireless networking of CRISP robots. It is possible to network these individual NodeMCU's wirelessly by integrating them with IoT in a smart manner. The data corresponding to the status of each robot along with its associated PV system parameters in CRISP can be accessed via NodeMCU by the user to store in cloud data base and can achieve desired control and monitoring operations using existing communication methodologies and techniques.

The NodeMCU module can be configured as a station, so as to connect it to the Wi-Fi network. It can also be configured as a soft access point (soft-AP), to establish its own Wi-Fi network. Therefore, it is possible to connect other stations to such NodeMCU module so that it exhibits the ability to operate both in station as well as soft access point mode. This provides the possibility of integrating a large network such as a star or mesh network by using the same network devices. Here the developed prototype assumes each NodeMCU as an individual CRISP and collects the data from requisite sensors discussed in previous section for monitoring and control. Different wireless networking topologies (star, radial and long range) are taken into design considerations based on NodeMCU and are presented as follows.

#### 3.1 Star topology

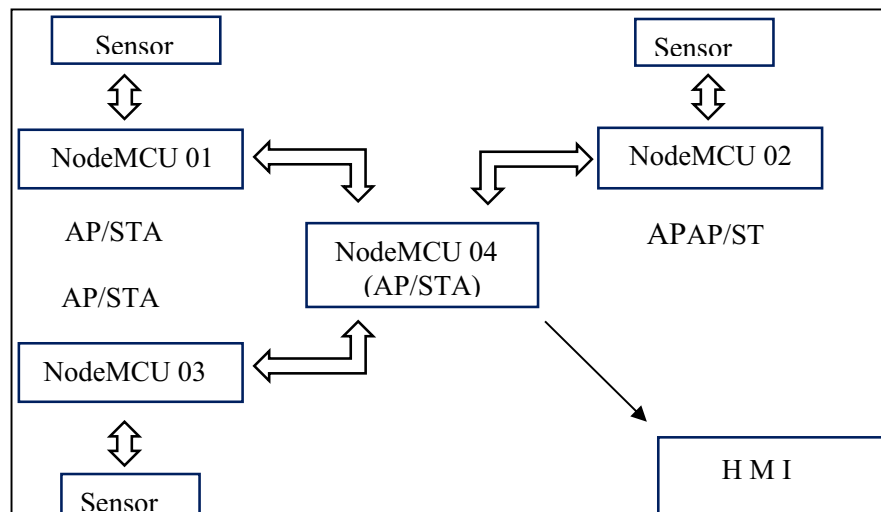


**Figure 3.** Basic structure of star topology.

The Digital Humidity and Temperature (DHT11) sensor is used in this topology to measure and transfer temperature and humidity data values, and in this network, the sensor can be powered ON and OFF from the monitor which is displayed in the HMI. Figure 3 above shows the basic structure of the wireless networking star topology. The network topology for controlling the robot and monitoring of temperature and humidity values of the DHT11 sensor can be explained with the help of following flow chart shown in figure 4.

Initially, all the NodeMCU's are configured in AP mode and the HMI is connected to the NodeMCU 04 with proper service set identifier (SSID) and Password. Once the connection is established, access the NodeMCU by calling its internet protocol (IP) address in the web page, then the user interface (UI) containing the home page will be shown on the HMI. Then select any one of the NodeMCU's to read the temperature and humidity values of the respective DHT by pressing the request button. Then the connected AP (NodeMCU 04) is configured as a station mode and it will connect to the selected NodeMCU and sends a request to it. Then the respective DHT is powered ON and will read and store the temperature and humidity values. Next, the selected NodeMCU is configured as a station mode and connects to the NodeMCU 04 and posts the temperature and humidity data. Then the DHT is powered OFF and the NodeMCU is configured as an access point (AP).

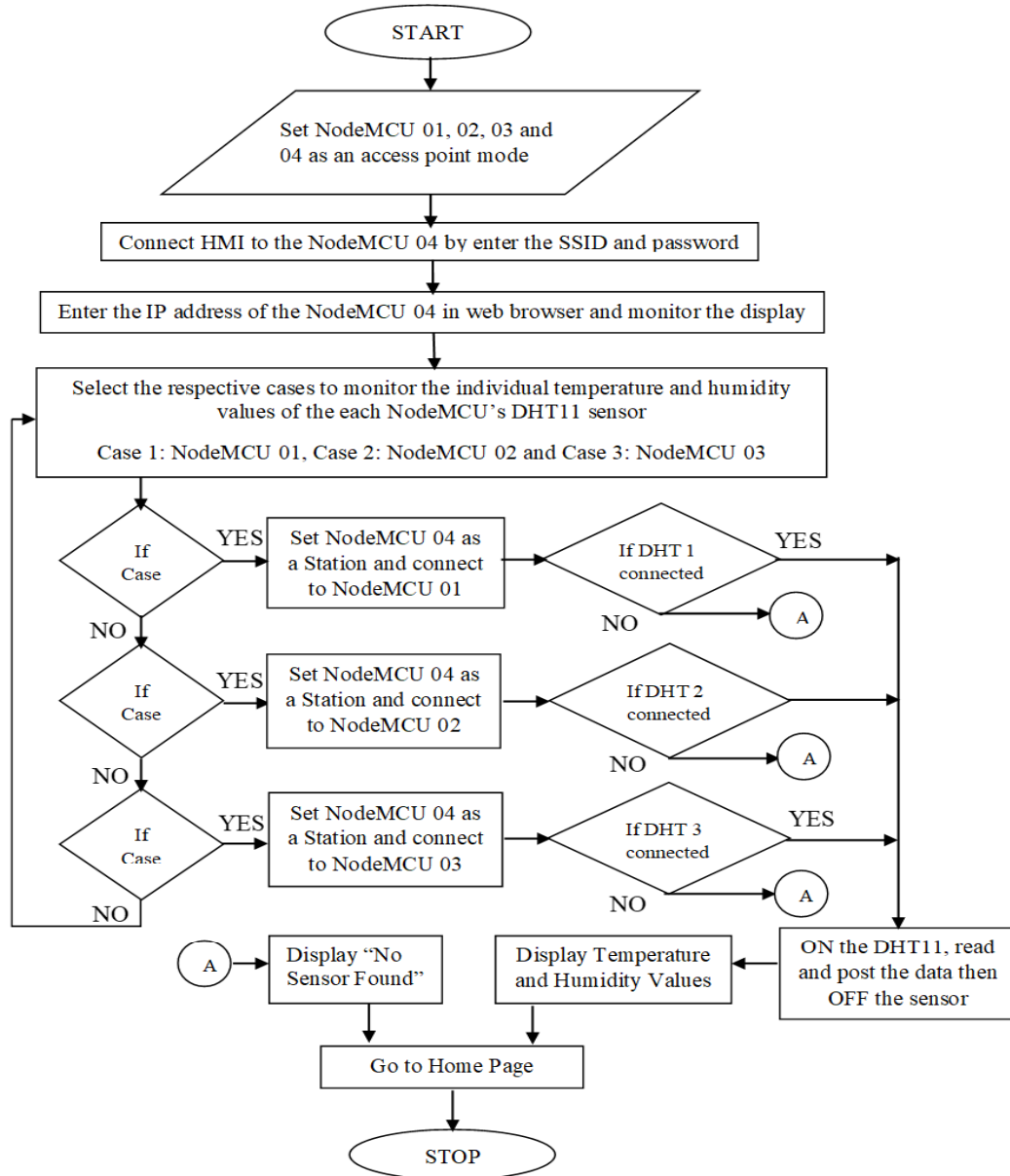


**Figure 4.** flow chart of star topology.

In the HMI monitor, whenever the read button is pressed, the temperature and humidity values will be appeared on a new page. If no DHT sensor is connected to the respective NodeMCU, “No Sensor Found” will appear on the screen. In this topology, the DHT sensor is OFF unless the request button of the respective NodeMCU on the home page is pressed. So, the power can be saved. This topology is used not only to read the temperature and humidity values on the monitor but also it will control the DHT sensor ON and OFF. With the reference of this topology, it can control the motors and LED to switch ON and OFF for emergency purpose. The next step in this topology is including the LED indicators and motors which are to be controlled either ON or OFF and display on the monitor to know the status. This topology’s range is less than 100 meters only and this topology support the users to control the robots individually. So this wireless network topology can be used for local area purpose.

### 3.2 Radial topology

In this topology, the NodeMCU's can be networked wirelessly in the form of a serial connection, so it is called radial topology. Where the NodeMCU 01 is not directly communicated with the HMI, it will communicate to the HMI through other NodeMCU's which means that the NodeMCU 01 will communicate with NodeMCU 02, and then it will communicate with NodeMCU 03 later it will communicate with NodeMCU 04. The process is reversed while the communication from HMI to NodeMCU 01. This topology is mainly suitable for long-range wireless networking. The one better thing in this topology is the medium NodeMCU also serves its own data along with the data of the adjacent NodeMCU to the HMI. And the NodeMCU 04 gathers the data from all the NodeMCU's and sends it to the HMI, at the same time it will also send the data of its own sensors.

In this wireless networking topology, data of all the NodeMCUs can be displayed on the same web page. So, this topology can be used to monitor all the NodeMCU's data on a single monitor at the same time. In this topology, the DHT11 sensor is used for the monitor and control from the HMI.

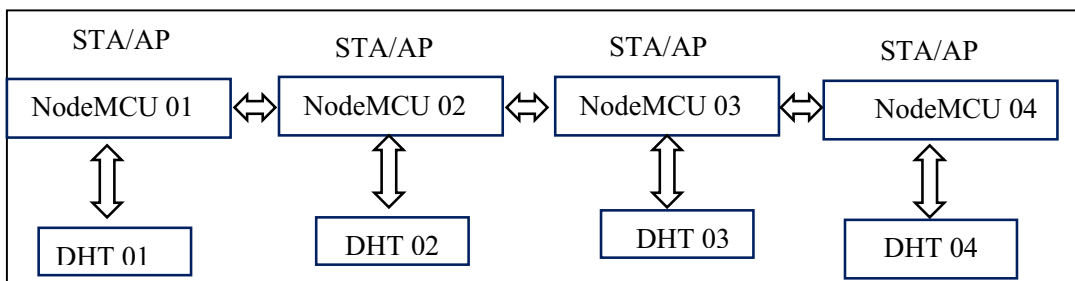


**Figure 5.** basic Structure of Radial topology.

Figure 5 shows a complete architecture of wireless networking with radial topology. In this topology, all the four NodeMCU's can be used to transfer the data to HMI. And if anyone sensor fails to prepare the weather report, then it will indicate on the monitor that the sensor is not found. Further, the DHT will not be powered ON until the Request is sent from the HMI. The complete network performance of radial wireless networking topology can be explained with the use of flow chart which is shown in figure 6. Initially, all the NodeMCU's are set up as an access point and the HMI will connect to the NodeMCU 04 by entering the proper SSID and Password. Then enter the IP address of the NodeMCU 04 in the web browser to display the home page on the monitor.

Whenever request button is pressed which is displayed on the monitor, the DHT4 sensor is Powered ON and measures the Temperature and Humidity values and stores it. Then the NodeMCU 04 sets up in STA mode and requests the NodeMCU 03 and is again set up as an AP. Then the NodeMCU 03 setup as an STA mode then connected to the NodeMCU 02 and the DHT3 sensor is Powered ON and it measures the Temperature values and stores it and again set up as an AP. Next, the NodeMCU 02 setup as an STA mode then connected to the NodeMCU 01 and the DHT2 sensor is Powered ON and it measures the Temperature values and stores it and again set up as an AP. Up next, the NodeMCU 01 DHT sensor is Powered ON and it measures the Temperature and humidity values and setup as an STA mode then connected to the NodeMCU 02 and transfers the data, DHT1 sensor Powered OFF and again set up as an AP.

The NodeMCU 02 receives the DHT01 data and adds it to the DHT02 data of temperature and humidity values and setup as an STA mode then connected to the NodeMCU 03 and transfers the data, DHT02 sensor powered OFF and again set up as an AP. Next, the NodeMCU 03 receives the DHT01 and DHT02 data and add it to the data of DHT03 and setup as an STA mode then connected to the NodeMCU 04 and transfer the data, DHT03 sensor powered OFF and again set up as an AP.

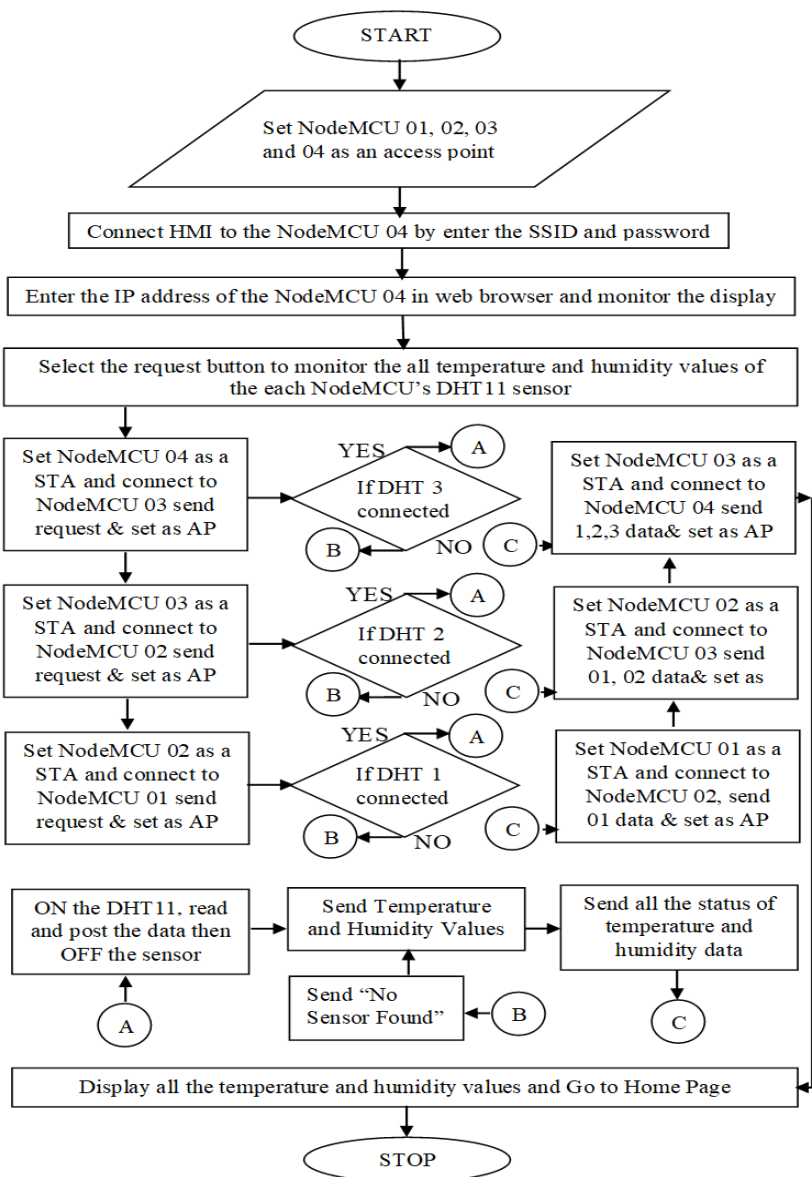


**Figure 6.** Flow chart of Radial topology

Finally, the NodeMCU 04 receives the DHT01, DHT02, and DHT03 data and adds it to the DHT04 data of Temperature and humidity values and stores it. Then, DHT04 powered OFF. So whenever Read button on the monitor is pressed, each DHT's measured value will be displayed on the new web page. Moreover, if any DHT is not connected to the NodeMCU, then it will show "No Sensor Found". This topology is suitable for long-range data transfer and control of application. In the next step, the motor and LED indicator can be included in this radial topology. To transfer the data in this topology, it will take the time delay to setup the AP or STA modes. So, this problem can be eliminated by the use of next topology with repeaters for long range.

### 3.3 long-range topology

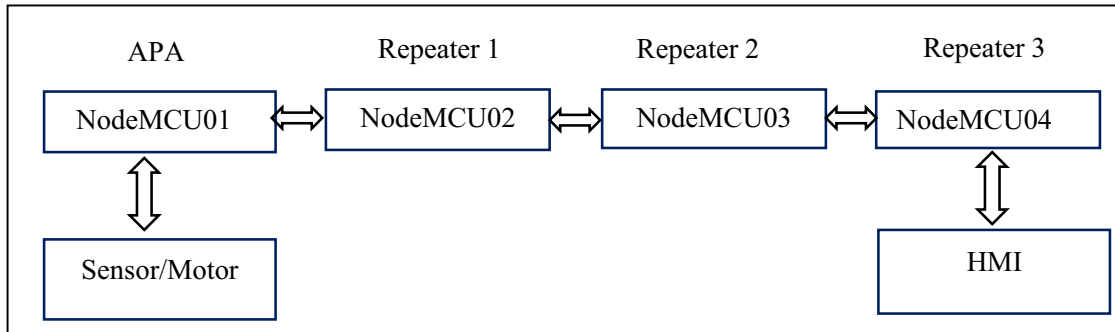


**Figure 7.** Basic structure of Long-range topology.

This topology is an advanced one which is being used for long-range applications with instant control and monitoring of the devices. Before starting this topology the NodeMCU is configured as a Repeater. While setup, it will ask the station mode and access point mode settings. In the AP settings, the SSID and Password can be set up for repeater. Whereas in STA settings, enter the SSID and Password of the other AP device which we want to connect to it. The repeater can be set up as an auto mesh mode to connect automatically to the nearest AP devices based on their signal strength. Figure 7 gives the basic structure of wireless networking with long-range topology by repeaters. Where the NodeMCU 01 as an access point and the DHT sensor, Motor and LED indicator are connected to it. In Repeater 1, the station (STA) SSID and Password belong to NodeMCU 01 and in Repeater 2, the STA SSID and Password belong to Repeater 1 and in Repeater 3, the STA SSID and Password belong to Repeater 2. Now the Repeater3 will give access to the HMI. Then the HMI can connect to any one of the Repeater to control and monitor the devices which are connected to the NodeMCU 01 based on the required range.

In this topology, power, speed and direction of the motor can be controlled, LED indicator power and brightness can be controlled and the weather report from the DHT sensor can be displayed. The complete working performance can be explained based on the flow chart which is shown in figure 8. Initially, the HMI is connected to the Repeater 3 or 2 or 1 based on the range we required with proper SSID and Password. After opening a web page and entering the IP address of NodeMCU 01, the web page will appear which include the weather report, motor control and LED control. There will be some buttons which are used to control the Motor and LED indicator. The weather report is updated for every refresh of the page. To control the Motor, ON and OFF buttons are provided to power it on and off. In addition, the direction of the motor can be controlled by pressing the ‘change direction button’ on the display. The speed control is also possible by pressing the increase and decrease buttons. For control of the LED indicator, ON and OFF buttons are provided to power the LED and the brightness of the LED can be increased or decreased by pressing respective buttons which are displayed on the HMI.

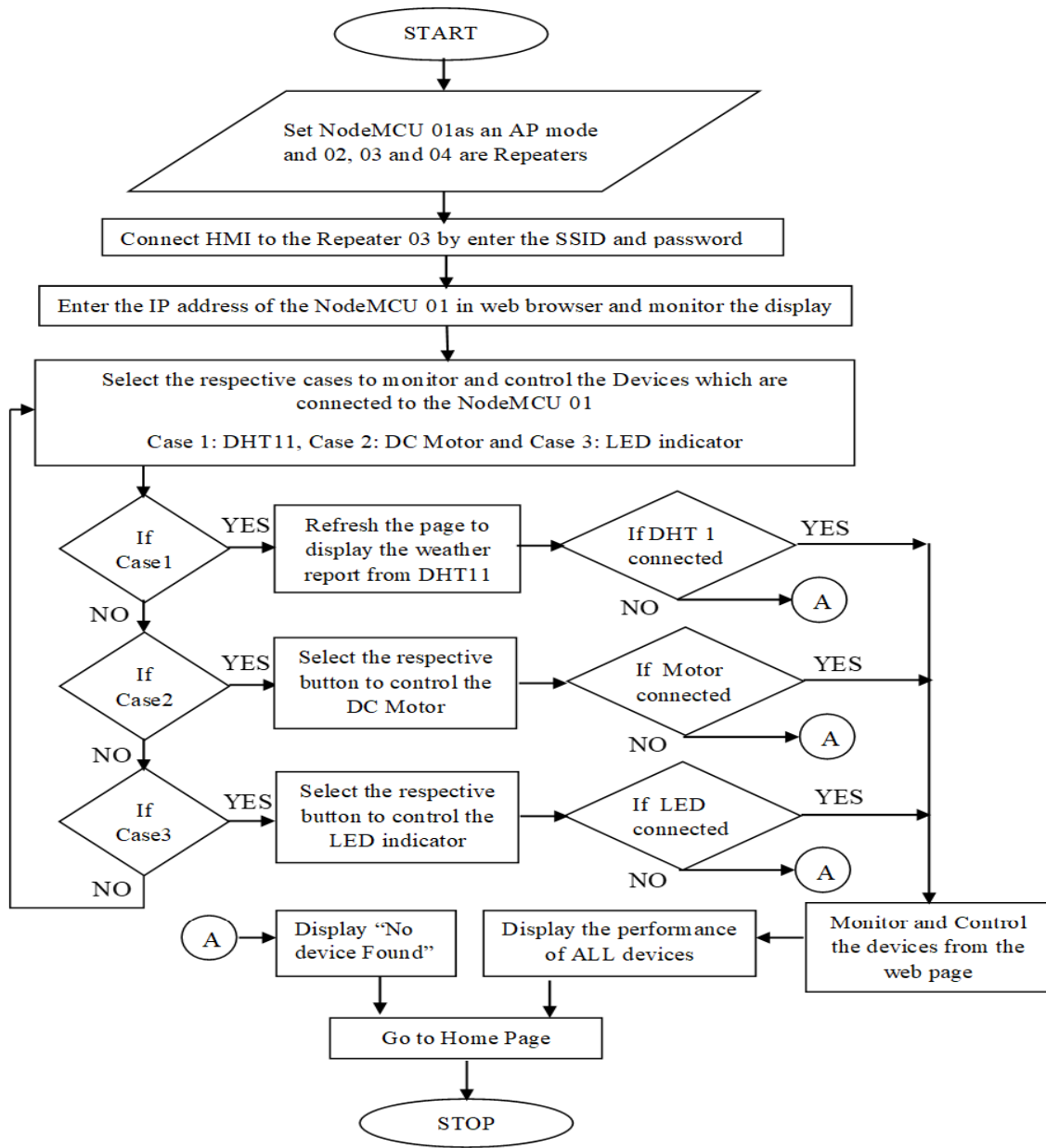


**Figure 8.** Flow chart of Long-range topology.

#### 4. Results and Discussion

Different types of wireless networking topologies are designed by considering star, radial and long-range topologies for development of CRISP at BHEL. The development procedure followed in successful development and implementation under Arduino IDE environment with ESP 8266 NodeMCU for star topology is presented in figure 9. Before starting the wireless networking of these devices, open the Arduino IDE software in PC and prepare the individual code to each NodeMCU. Then all the NodeMCU's are fixed to the breadboard and connected to the PC through the USB cable. Also, connect the DHT11 sensors to the

NodeMCU's with respective pins as per the code. In this topology, the DHT11 is not connected to the NodeMCU 03 to check the variation with NodeMCU's connected with DHT11. After connections, select the respective ports and upload the code which is written in the software. In this topology, the range from each NodeMCU to Access Point is 50 meters but those all are placed near to each other to understand how the data is being transferred and controlled through the serial monitor. After uploading the code into the respective NodeMCU's, open the serial monitor. Now connect the HMI to the NodeMCU 04 by entering the proper SSID and Password. Then open the web browser and type the IP address of NodeMCU 04 (192.168.4.4), then the web page will appear which is shown in figure 10. The results of star topology can be studied under two scenarios which are based on whether the DHT11 is connected to NodeMCU or not.

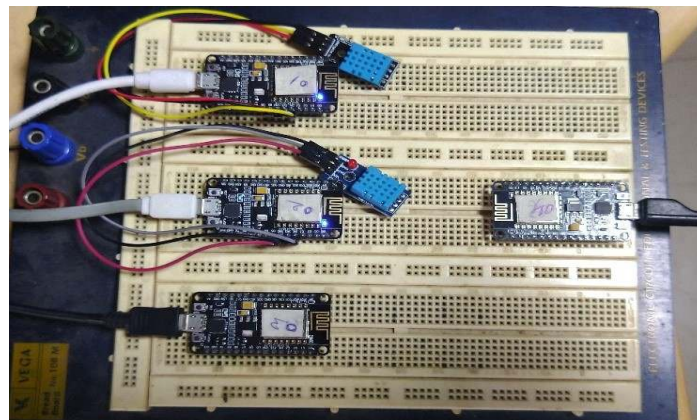


**Figure 9.** Wireless networking with a star topology.

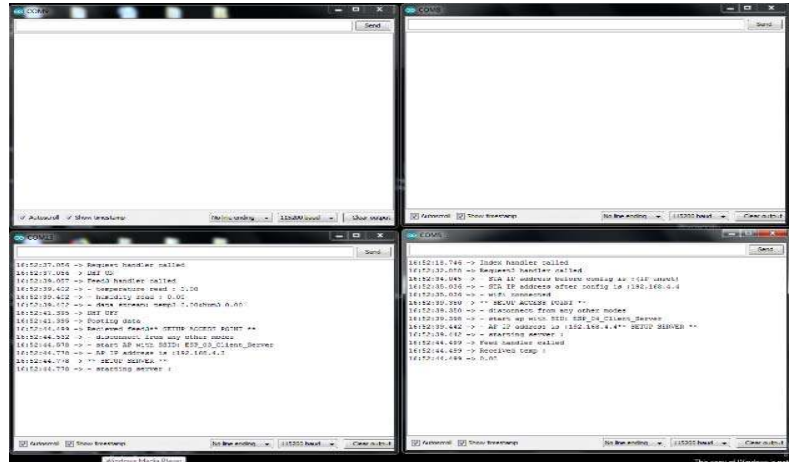


**Figure 10.** Home page for star topology.

In case 1, the DHT11 is not connected to the NodeMCU 03, so it should display “No Sensor Found”. So, whenever we press the REQUEST3 button on the home page it will send the request to the NodeMCU 03 but here no sensor is connected to NodeMCU, so it will show “No Sensor Found” which is shown in figure 11b. This web page can be obtained by pressing the READ3 button on the home page. From figure 11a, clearly shows the data transfer and control mechanism of DHT11 sensor between Access Point and NodeMCU 03.

In case 2, the DHT11 is connected to the NodeMCU 01 to display the temperature and humidity values. By clicking on REQUEST1 button on the home page, request is initiated at NodeMCU 01 and turns ON the DHT11 which sends the requisite data pertaining to temperature and humidity on LCD display by

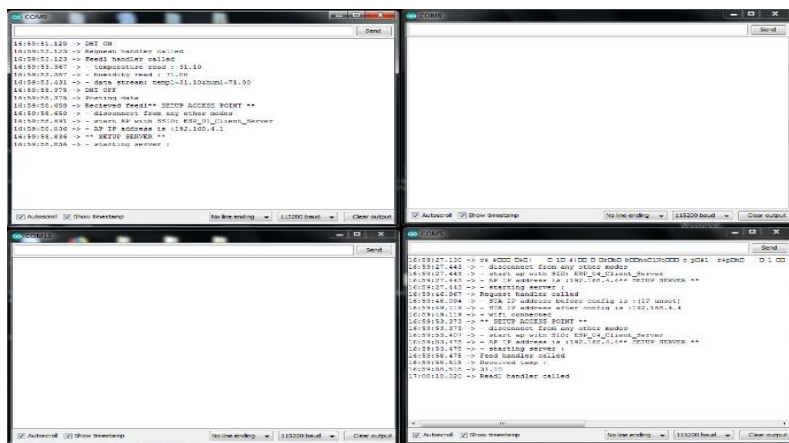
pressing the READ1 button on the home page as shown in figure 12b while figure 12a clearly shows the data transfer between Access Point and NodeMCU 01 to control DHT11 sensor.



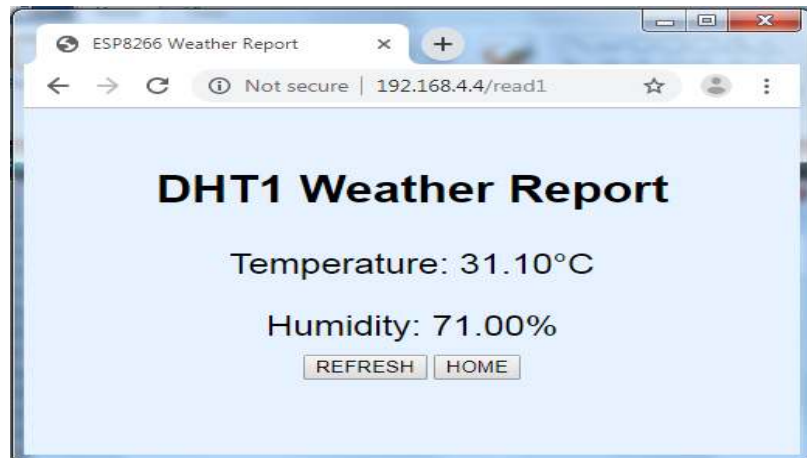
**Figure 11.** Star topology NodeMCU 03 results (a) Serial monitor.



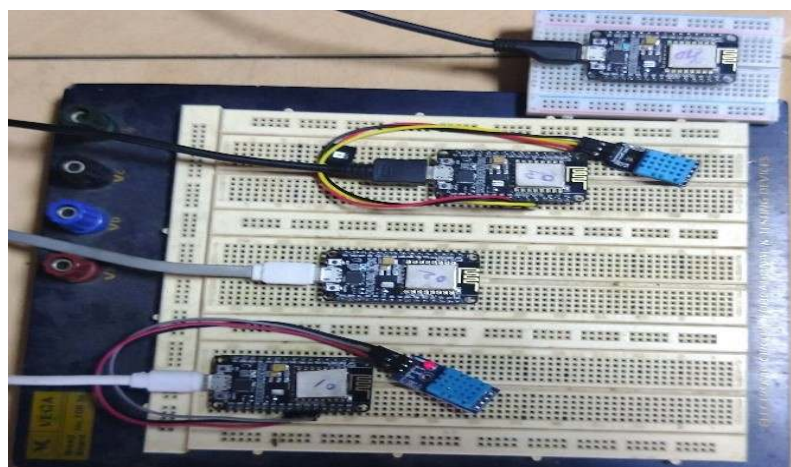
(b) Web page.



**Figure 12.** Star topology NodeMCU 01 results (a) Serial monitor.



(b) Web page.

**Figure 13.** Wireless networking with radial topology.**Figure 14.** Home page for radial topology.

Radial topology is an extension to star topology to increase the range of wireless networking. In radial topology, four NodeMCU's and two DHT11 sensors are used for wireless networking and those are connected in a radial topology as shown in figure 13. Here in this topology all the four NodeMCU's were considered as a robot and the fourth NodeMCU is used as an access point to establish communication between individual NodeMCU's and central control station.

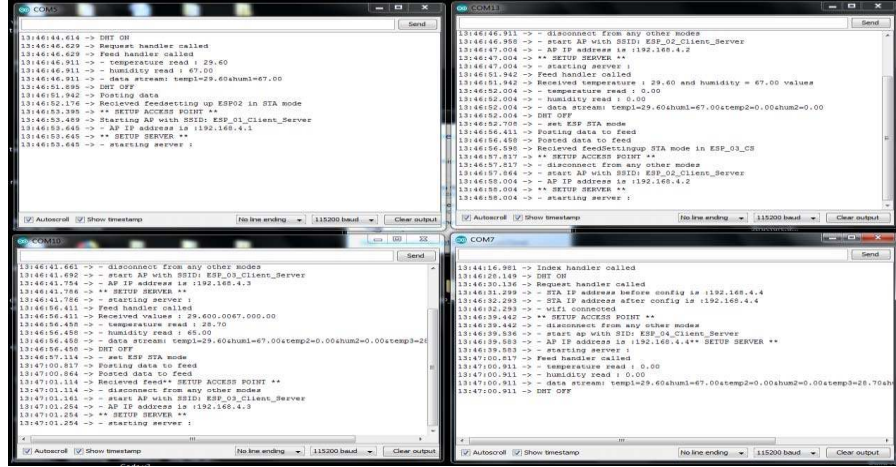


**Figure 15.** Radial topology results (a) Serial monitor.



(b) Web page.

The development procedure followed in successful development and implementation under Arduino IDE environment with ESP 8266 NodeMCU for radial topology initially starts by opening the Arduino IDE software in PC and prepare the individual code to each NodeMCU before starting the wireless networking of these devices. By using the USB cable, connect all the NodeMCUs which are fixed on the breadboard to the PC. Then connect the DHT11 sensors to the NodeMCU's with respective pins as mentioned in the code. In this topology also, the DHT11 is not connected to the NodeMCU02 and NodeMCU04 to check the variation with connected NodeMCU's. After connections, select the respective ports and upload the code which is written in the software. The range from each NodeMCU to AP is selected as 50 meters but for the sake of convenience all the NodeMCU's were placed nearer to each other to understand how the data is being transferred and DHT11 is controlled through the serial monitor. After uploading the code into the respective NodeMCUs, open the serial monitor and select Wi-Fi mode on devices and connect to the NodeMCU 04 by providing access to connect it by entering the proper SSID and

Password. Then open the web browser and type the IP address of NodeMCU 04 (192.168.4.4) which displays the web page as shown in figure 14. The results of this radial wireless networking topology can be monitored on the web page and with the help of a serial monitor, it can be observed that how the data can be transferred from NodeMCU 01 to NodeMCU 04 or vice versa.

By pressing the REQUEST button on the home page, the request can be sent from NodeMCU 04 to NodeMCU 01. The DHT11 sensors will be powered ON and start to send the data to the NodeMCU 04 through the NodeMCU 02 and NodeMCU 03. The NodeMCU 03 transfers the data of its DHT11 sensor along with NodeMCU01 data. Similarly, the NodeMCU02 transfers the data of its DHT11sensor data along with NodeMCU 01 and NodeMCU 02 sensors data. Finally, the NodeMCU 04 gets all the sensors data and adds its sensor data to them and stores it in a string. Then the DHT11 sensors will be powered OFF which is shown in figure 15a. And by pressing the READ button on the home page, the weather report will be displayed on the new web page which is shown in figure 15b. In this topology, the DHT11 sensors are not connected to the NodeMCU02 and NodeMCU 04. So only the temperature and humidity values of NodeMCU 01 and NodeMCU 03 are displayed. For NodeMCU 02 and NodeMCU 04, “No Sensor Found” is displayed. Although the range can be extended in radial network topology, the data transfer delay is a serious concern of about 8 to 10 seconds. So, in order to overcome this problem, the repeaters can be used as a medium to transfer the data from NodeMCU 01 to HMI. In this topology, the NodeMCU 01 consists of DHT11 sensor, LED indicator and one DC motor driver which are shown in figure 16.

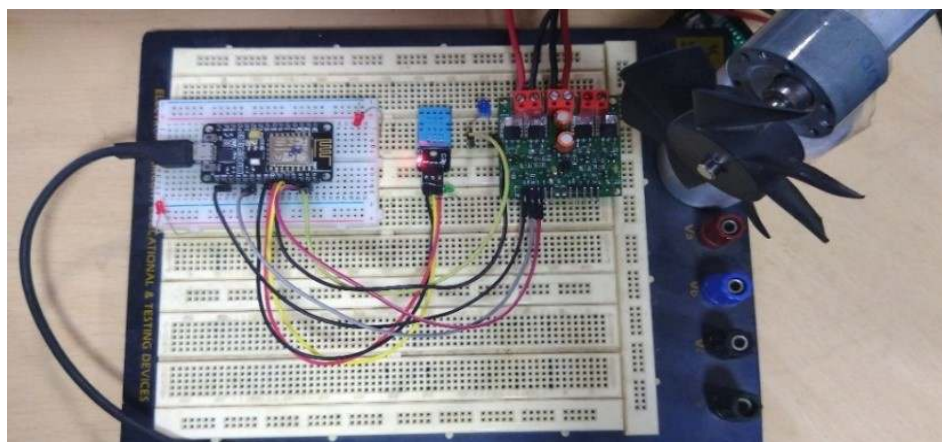


**Figure 16.** Wireless networking with long-range topology.

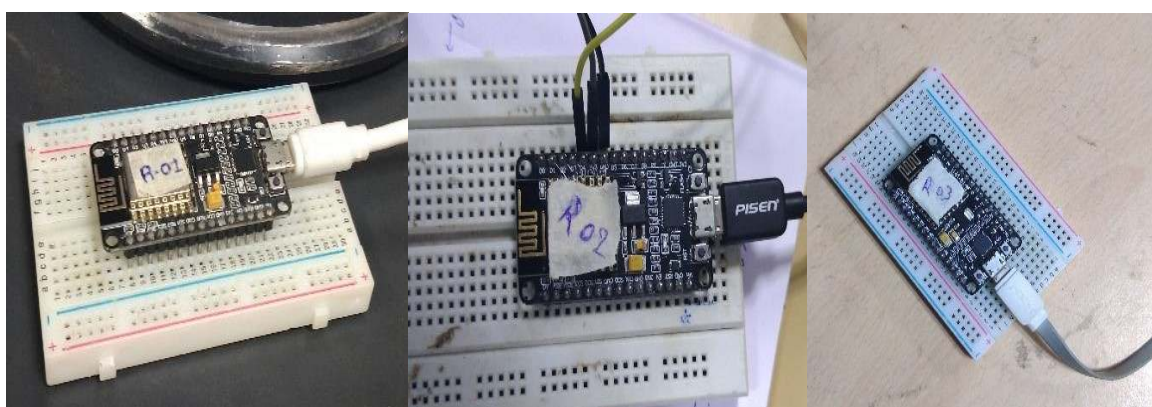


**Figure 17.** Repeaters 01, 02 and 03 at different locations.

Long range topology consists of three repeaters which are used to increase the range of the wireless network and operate the devices which are connected to the NodeMCU instantly. The developmental procedure can be initiated by preparing the requisite code for NodeMCU 01 in Arduino IDE software environment and then connecting NodeMCU 01 to the PC through USB cable followed by allowing all the devices to get connected to NodeMCU 01 pins as per the code configuration of the software thereby port selection and code launching can be carried out. Now configure the other three NodeMCU's as repeaters using Flash Downloader tool provided by espressif which are shown in figure 17. While configuring as a repeater, it should be reminded that STA has to be setup followed by AP settings in which the SSID and Password in STA settings are similar to that of SSID and Password of other NodeMCU's which provides access to it. For this topology, the three repeaters are placed at different locations in transmission and distribution laboratory (TDL) at BHEL by maintaining a distance of about 50 to 70 meters between every two repeaters. Now the power is allowed to each repeater with a USB cable to attain access to other stations and connect the HMI to the repeater 03 by entering proper SSID and Password. Next, go to a web browser and type the IP address of NodeMCU 01 (192.168.4.4) to display relevant web page as shown in figure 18.

The results of long-range repeaters can be obtained instantly on web page wherein the weather report from the DHT11 sensor can be updated and displayed for every refresh of the web page. The motor can be controlled in three ways i.e. switching the power supply in ON and OFF conditions for motor operation, by changing the direction of shaft rotation, and controlling the speed of the motor either by increasing or decreasing. The LED can be controlled in two ways i.e. by switching the power supply in ON and OFF conditions and by increasing or decreasing the brightness of the LED. The devices can be controlled by pressing the respective buttons on the web page.



**Figure 18.** Home page for long-range topology.

## 5. Conclusion

The main objective of this work is to provide wireless networking for the solar panel cleaning robots which are used to clean the dust accumulated on the solar panel. This work emphasizes on the development of CRISP robot to control and monitor robots from a long distance by establishing a network of many robots connected to a central control station. The CRISP is developed to overcome the problem of

accumulation of dust on the solar panel with advanced technology and better performance at BHEL Hyderabad. It is controlled wirelessly using Wi-Fi from the HMI. Different wireless networking topologies are designed and developed by utilizing NodeMCU as microcontroller and Wi-Fi device for CRISP. Replacement of PLC and Wi-Fi router in CRISP with NodeMCU showed significant reduction on incurred capital.

In star topology, all the robots are wireless networked to one NodeMCU which is an access point interconnected with HMI to control each robot individually. Using this topology, it has been identified that the robots were controlled within a limited range i.e. about 50 to 70 meters from the access point. To increase the range of the wireless network the radial topology was developed where the range of wireless networking was increased from 50 meters to 200 meters with the help of three more NodeMCU's. Those three NodeMCU's are used not only to increase the range of the network but also made to control an individual robot. But a delay of around 4 seconds was observed between each NodeMCU of the network. As these are networked in serial format, to control and monitor the NodeMCU 01, it takes around 15 seconds. To overcome this problem, long-range wireless networking topology was taken into consideration wherein the repeaters (additional NodeMCU's) are introduced for wireless networking of the robots. By setting up the STA and AP settings in repeaters, wireless network coverage can be enhanced to the desired level over a long distance so that demerits of previous two topologies can be minimized.

The work can be further improvised by utilizing wireless networking with a mesh topology for CRISP robots which are used in large solar power plants and supplemental wireless bypass networking topology in which, if one NodeMCU fails to connect to the next NodeMCU, it connects to the next available NodeMCU to maintain the network. The NodeMCU has only one analog read pin which can be extended with the multiplexer. Extension of these wireless networking topologies to other similar products like street light controlling can also be considered towards networking with smart grid operations. Hence, it can be concluded that utilization of CRISP with appropriate wireless networking topology for monitoring and control of solar PV panel cleaning in an efficient manner will remain as a viable option for industrial scale large solar power plants.

**Acknowledgments:** The authors express their gratitude to the BHEL R&D Division, Hyderabad; JNT University, Kakinada and Centre for Smart Grid Technologies, Vellore Institute of Technology, Vellore, India for their entire support towards this research work.

## References

- [1]. Sitharthan R, Geethanjali M and Pandey TKS 2016 Adaptive protection scheme for smart microgrid with electronically coupled distributed generations *Alexandria Engineering Journal* **55**(3) 2539-2550
- [2]. Fathima AH, and Palanisamy K 2014 Battery energy storage applications in wind integrated systems—a review *IEEE International Conference on Smart Electric Grid* 1-8
- [3]. Prabaharan N and Palanisamy K 2015 Investigation of single-phase reduced switch count asymmetric multilevel inverter using advanced pulse width modulation technique *International Journal of Renewable Energy Research* **5**(3) 879-890.
- [4]. Jerin ARA, Kaliannan P and Subramaniam U 2017 Improved fault ride through capability of DFIG based wind turbines using synchronous reference frame control based dynamic voltage restorer. *ISA transactions* **70** 465-474
- [5]. Sitharthan, R, Sundarabalan CK, Devabalaji KR, Nataraj SK and Karthikeyan M 2018 Improved fault ride through capability of DFIG-wind turbines using customized dynamic voltage restorer *Sustainable cities and society* **39** 114-125
- [6]. Prabaharan N and Palanisamy K 2016 A single-phase grid connected hybrid multilevel inverter for interfacing photo-voltaic system *Energy Procedia* **103** 250-255

- [7]. Palanisamy K, Mishra JS, Raglend IJ and Kothari DP 2010 Instantaneous power theory based unified power quality conditioner (UPQC) *IEEE Joint International Conference on Power Electronics, Drives and Energy Systems* 1-5
- [8]. Sitharthan R and Geethanjali M 2017 An adaptive Elman neural network with C-PSO learning algorithm-based pitch angle controller for DFIG based WECS *Journal of Vibration and Control* **23**(5) 716-730
- [9]. Sitharthan R and Geethanjali M 2015 Application of the superconducting fault current limiter strategy to improve the fault ride-through capability of a doubly-fed induction generator-based wind energy conversion system *Simulation* **91**(12) 1081-1087
- [10]. Sitharthan R, Karthikeyan M, Sundar DS and Rajasekaran S 2020 Adaptive hybrid intelligent MPPT controller to approximate effectual wind speed and optimal rotor speed of variable speed wind turbine *ISA transactions* **96** 479-489
- [11]. Sitharthan R, Devabalaji KR and Jees A 2017 An Levenberg–Marquardt trained feed-forward back-propagation based intelligent pitch angle controller for wind generation system *Renewable Energy Focus* **22** 24-32
- [12]. Sitharthan R, Sundarabalan CK, Devabalaji KR, Yuvaraj T and Mohamed Imran A 2019 Automated power management strategy for wind power generation system using pitch angle controller *Measurement and Control* **52**(3-4) 169-182
- [13]. Sundar DS, Umamaheswari C, Sridarshini T, Karthikeyan M, Sitharthan R, Raja AS and Carrasco MF 2019 Compact four-port circulator based on 2D photonic crystals with a 90° rotation of the light wave for photonic integrated circuits applications *Laser Physics* **29**(6) 066201
- [14]. Sitharthan R, Parthasarathy T, Sheeba Rani S and Ramya KC 2019. An improved radial basis function neural network control strategy-based maximum power point tracking controller for wind power generation system *Transactions of the Institute of Measurement and Control* **41**(11) 3158-3170
- [15]. Rajesh M and Gnanasekar JM 2017 Path observation based physical routing protocol for wireless ad hoc networks *Wireless Personal Communications* **97**(1) 1267-1289
- [16]. Palanisamy K, Varghese LJ, Raglend IJ and Kothari DP 2009. Comparison of intelligent techniques to solve economic load dispatch problem with line flow constraints *IEEE International Advance Computing Conference* 446-452
- [17]. Sitharthan R, Ponnusamy M, Karthikeyan M and Sundar DS 2019 Analysis on smart material suitable for autogenous microelectronic application *Materials Research Express* **6**(10) 105709
- [18]. Rajaram R, Palanisamy K, Ramasamy S and Ramanathan P 2014 Selective harmonic elimination in PWM inverter using fire fly and fireworks algorithm *International Journal of Innovative Research in Advanced Engineering* **1**(8) 55-62
- [19]. Sitharthan R, Swaminathan JN and Parthasarathy T 2018 March. Exploration of wind energy in India: A short review *IEEE National Power Engineering Conference* 1-5
- [20]. Karthikeyan M, Sitharthan R, Ali T and Roy B 2020 Compact multiband CPW fed monopole antenna with square ring and T-shaped strips *Microwave and Optical Technology Letters* **62**(2) 926-932
- [21]. Sundar D Sridarshini T, Sitharthan R, Madurakavi Karthikeyan, Sivanantha Raja A, and Marcos Flores Carrasco 2019 Performance investigation of 16/32-channel DWDM PON and long-reach PON systems using an ASE noise source *In Advances in Optoelectronic Technology and Industry Development: Proceedings of the 12th International Symposium on Photonics and Optoelectronics* 93
- [22]. Sitharthan R and Geethanjali M 2014 Wind Energy Utilization in India: A Review *Middle-East J. Sci. Res.* **22** 796–801 doi:10.5829/idosi.mejsr.2014.22.06.21944

- [23]. Sitharthan R and Geethanjali M 2014 ANFIS based wind speed sensor-less MPPT controller for variable speed wind energy conversion systems *Australian Journal of Basic and Applied Sciences* **8** 14-23
- [24]. Jerin ARA, Kaliannan P, Subramaniam U and El Moursi MS 2018 Review on FRT solutions for improving transient stability in DFIG-WTs *IET Renewable Power Generation* **12(15)** 1786-1799
- [25]. Prabaharan N, Jerin ARA, Palanisamy K and Umashankar S 2017 Integration of single-phase reduced switch multilevel inverter topology for grid connected photovoltaic system *Energy Procedia* **138** 1177-1183
- [26]. Rameshkumar K, Indragandhi V, Palanisamy K and Arunkumari T 2017 Model predictive current control of single phase shunt active power filter *Energy Procedia* **117** 658-665
- [27]. Fathima AH and Palanisamy K 2016 Energy storage systems for energy management of renewables in distributed generation systems *Energy Management of Distributed Generation Systems* 157
- [28]. Rajesh M 2020 Streamlining Radio Network Organizing Enlargement Towards Microcellular Frameworks *Wireless Personal Communications* 1-13
- [29]. Subbiah B, Obaidat MS, Sriram S, Manoharn R and Chandrasekaran SK 2020 Selection of intermediate routes for secure data communication systems using graph theory application and grey wolf optimisation algorithm in MANETs *IET Networks* doi:10.1049/iet-net.2020.0051
- [30]. Singh RR and Chelliah TR 2017 Enforcement of cost-effective energy conservation on single-fed asynchronous machine using a novel switching strategy *Energy* **126** 179-191
- [31]. Amalorpavaraj RAJ, Palanisamy K, Umashankar S and Thirumoorthy AD 2016 Power quality improvement of grid connected wind farms through voltage restoration using dynamic voltage restorer *International Journal of Renewable Energy Research* **6(1)** 53-60
- [32]. Singh RR, Chelliah TR, Khare D and Ramesh US 2016 November. Energy saving strategy on electric propulsion system integrated with doubly fed asynchronous motors *IEEE Power India International Conference* 1-6
- [33]. Sujatha K and Punithavathani DS 2018 Optimized ensemble decision-based multi-focus imagefusion using binary genetic Grey-Wolf optimizer in camera sensor networks *Multimedia Tools and Applications* **77(2)** 1735-1759
- [34]. Krishnamoorthy S, Punithavathani S and Priya JK 2017 Extraction of well-exposed pixels for image fusion with a sub-banding technique for high dynamic range images *International Journal of Image and Data Fusion* **8(1)** 54-72
- [35]. Singh RR, Mohan H and Chelliah TR 2016 November. Performance of doubly fed machines influenced to electrical perturbation in pumped storage plant-a comparative electromechanical analysis *IEEE 7th India International Conference on Power Electronics* 1-6